ROTATIONAL TRANSITIONS IN THE ELECTRON-IMPACT IONIZATION OF NITROGEN IN THE $N_2^+ (B^2\Sigma_u^+,\ v' = 0)$ STATE

A. E. Belikov, A. I. Sedel'nikov, G. I. Sukhinin, and R. G. Sharafutdinov

UDC 537.525.533.6.011

Vibronic-state excitation in a molecule or molecular ion on electron impact is accompanied by change in the rotational state. One needs to know the transition probabilities for calculations on electroionization and gas-discharge lasers and to examine distributions over excited states in molecular plasmas, discharges, the ionosphere, etc. One determines the transition probabilities from vibrational-band structure, gas temperature, and level populations as determined by spectroscopic methods or by electron-beam diagnosis.

It has often been supposed since [1] that optical selection rules apply in electron-impact excitation; it is also assumed that the rotational distributions match in transitions from the ground state to excited ones [2, 3] on the basis that there cannot be any large change in the momentum on electron collision because of the small electron mass, and therefore the rotational-level distribution in the upper electronic state is almost the same as in the ground state [2]. However, recently it has been shown that electron-impact excitation for H_2 and N_2 involves considerable momentum transfer [4-6], and this increases as the exciting electron energy falls [7-9]. It is therefore necessary to determine the rotational transition cross sections for electron-impact excitation, which is complicated in theoretical and experimental respects. The theory at present does not enable one to determine the cross sections or probabilities in closed form for vibronic excitation by high-energy electrons, but the adiabatic approximation or the sudden-collision one [10-12] has given useful relations between the rotational transition cross sections: the entire cross section matrix can be expressed via the vector for the cross sections for transitions from the zero rotational level and the 3_j Wigner symbols.

When these transition probabilities are measured, it is necessary to provide a gas target having a known rotational-level distribution in the ground (initial) state and to measure the distribution in the excited one, which can be handled by spectroscopic methods if the excited state has a short lifetime and is linked by optical transitions to lower-lying states.

We chose nitrogen because it is a major atmospheric component and its electron-impact excitation is important for many processes in the ionosphere and upper atmosphere, while it is also a component of many gas-discharge and electroionization lasers.

1. We examined

$$N_2(X^1\Sigma_g^+) + e_b \rightarrow N_2^+(B^2\Sigma_u^+) + e_b + e_s$$
$$\downarrow$$
$$N_2^+(X^1\Sigma_g^+) + h\nu,$$

where e_b represents an electron with energy 10 keV and $h\nu$ is the emission in the first negative system 1NS. The gas target was provided by the nitrogen flow at the axis of a stationary free jet at low density formed by expansion into a vacuum chamber. The electron beam met it at right angles. The emission was collected from the small intersection region and recorded by a spectrometer. We used a gas-dynamic system at the Thermophysics Institute, Siberian Division, USSR Academy of Sciences [13], while the methods have been described in [5]. Figure 1 shows an example of the resolved 0–0 band in the first negative system ($N_2^+(B^2\Sigma_u^+,\ v' = 0,\ k') \rightarrow N_2^+(X^2\Sigma_g^+,\ v'' = 0, k'')$, transitions) excited by the electron beam. In accordance with the selection rule $\Delta k = k' - k'' = \pm 1$, there are two branches: the R branch ($\Delta k = -1$) and the P

Novosibirsk. Translated from Zhurnal Prikladnoi Mekhaniki i Tekhnicheskoi Fiziki, No. 3, pp. 3-14, May-June, 1988. Original article submitted February 10, 1987.

0021-8944/88/2903-0317$12.50

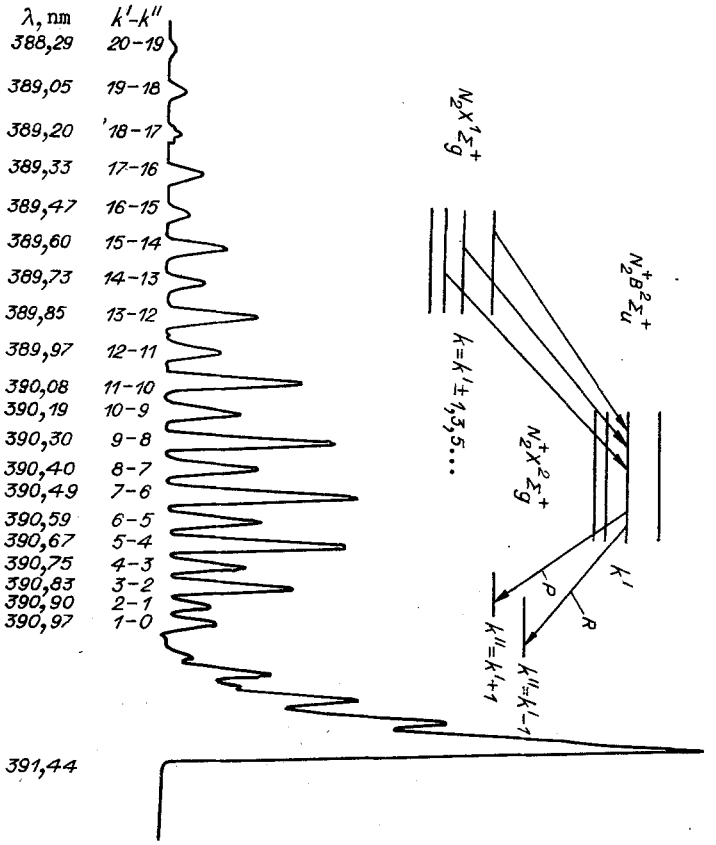

Fig. 1

branch ($\Delta k = 1$). A head is formed in the P branch, and the lines in that branch are poorly resolved, so we subsequently used the R lines and the first line in the P branch having $k' = 0$ and $k'' = 1$. There is intensity alternation associated with the nuclear spin [2].

The $N_2^+(B^2\Sigma_u^+)$ state is excited [5] by direct electron impact from the neutral molecule in the $N_2(X^1\Sigma_g^+, v=0)$ state. Figure 1 shows the rotational-transition scheme in the excitation and emission. The k' levels are excited from the k levels in accordance with the selection rules $\Delta k = k' - k = \pm 1, 3, 5, \ldots$ because nitrogen has a homonuclear molecule and transitions between levels identical in parity are strictly forbidden [2]. If the density is low enough, the levels are depleted only by spontaneous emission; the contribution to $N_2^+(B^2\Sigma_u^+)$ excitation from secondary electrons is small, and there is only a minor effect from fluorescence quenching. Then the expressions for the rotational-line intensities are [14]

$$I_{k'}^R = C\frac{k'}{2k'+1}N_{k'}^B,\quad I_{k'}^P = C\frac{k'+1}{2k'+1}N_{k'}^B. \tag{1.1}$$

Under stationary conditions,

$$N_{k'}^B = \sum_k P_{k'k}^{BX}(E_b)\,N_k^X. \tag{1.2}$$

The constant C includes all the quantities independent of k and k', including the beam current and the gas density; the superscripts R and P denote the R and P branch lines, $N_{k'}^B$ are the rotational-level populations in the $N_2^+(B^2\Sigma_u^+, v'=0)$ state, N_k^X the same in $N_2(X^1\Sigma_g^+, v=0)$, and $P_{k'k}^{BX}$ the rotational transition probabilities on excitation from the $N_2(X^1\Sigma_g^+, v=0, k)$ state by electron impact to $N_2^+(B^2\Sigma_u^+, v'=0, k')$.

2. The $P_{k'k}^{BX}$ can be determined by measuring the line intensities $I_{k'}$ and producing a known population distribution N_k^X in the ground state, as is evident from the [1, 2] expressions. In principle, the N_k^X can be determined under any conditions from additional measurements such as in laser-induced fluorescence [15] or in spontaneous or induced Raman scattering [16, 17]. Unfortunately, these methods are at present too complicated for use. We

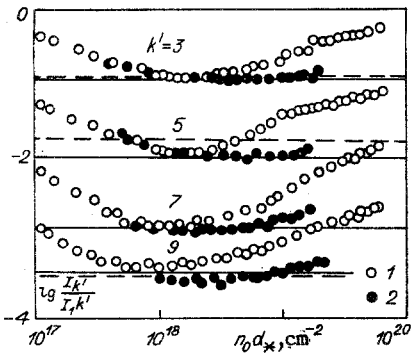

Fig. 2

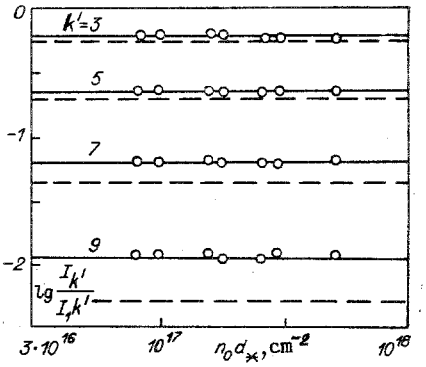

Fig. 3

obtained known distributions by providing equilibrium conditions at the axis of the free low-density jet. The N_k^X were derived from a Boltzmann distribution having a temperature derived by calculation on equilibrium isentropic expansion into vacuum [18]. Gas target preparation has two parts: 1) defining conditions in the jet such that the N_k^X have an equilibrium distribution but the gas density is low enough for one to neglect secondary processes and fluorescence quenching, and 2) demonstrating that one can use a theoretical calculation on the expansion to determine the axial temperature.

A free jet readily provides low translational temperatures in the range from a few degrees to a few tens of degrees Kelvin, but then the gas is below the saturation curve, i.e., supercooled. The state is affected by nonequilibrium condensation, which deposits energy, and the condensation also influences the rotational-level population kinetics [19]; so producing an equilibrium low-temperature distribution is complicated by the need to ensure that there is no condensation. These conditions were determined here by experiment.

The above distribution is produced as follows. If there is no condensation, the rotational relaxation is dependent on binary collisions. The distribution tends to equilibrium as the collisional frequency increases, which in turn is provided by an increase in $n_0 d_*$, where n_0 is the gas density in the forechamber (retardation density) and d_* is the critical section diameter in the nozzle. The N_k^X attain their equilibrium values at a given point as $n_0 d_*$ increases at constant retardation temperature T_0 in a way that can be checked by measurement on the rotational structure in the INS spectra. From (1.1) and (1.2) we see that the relative rotational-line intensities should tend to constants defined by the constant populations N_k^X, but this occurs only if there are no secondary processes or condensation.

Figure 2 shows measurements on the rotational-line intensities $I_{k'}^R$ as functions of $n_0 d_*$ for a nozzle having $d_* = 0.54$ mm, which were made at the axis at $x/d_* = 38$ and $T_0 = 295$ K (points 1). As $n_0 d_*$ increases, the relative intensities at first fall towards a certain limit, which is determined by the N_k^X corresponding to the calculated isentropic temperature for that x/d_*, with the limit in Fig. 2 represented by the solid lines and determined by the use of the $P_{k'k}^{BX}$ derived below. That behavior is due to rotational relaxation. However, as $n_0 d_*$ increases further, the intensities increase because condensation energy is deposited. Figure 2 shows that this nozzle with pure nitrogen does not give a region reasonably extended in $n_0 d_*$ where the intensity distribution is independent of the latter, and therefore the N_k^X attain their equilibrium values. At the same time, with the same $n_0 d_*$ but $d_* = 5.11$ mm (points 2), where the density is lower, i.e., condensation is less prominent and secondary processes are less important, we obtained a short range having constant relative intensities, and it is suggested that the N_k^X should attain their equilibrium values there.

More definite evidence was obtained with argon containing a little nitrogen (less than 5%). Figure 3 gives the intensities at the nozzle axis for $x/d_* = 1.67$, isentropic temperature $T = 44$ K, measurement made with $d_* = 15$ mm and $T_0 = 290$ K. There was a broad range in $n_0 d_*$ where the intensity distribution was independent of the latter and therefore there was more basis to take the N_k^X distribution as equilibrium (the dashed lines in Figs. 2 and 3 are the $I_{k'}$ calculated from the [1] model).

We always derived the equilibrium N_k^X on the assumption that the isentropic calculation applied at the axis. Without entering into the complicated question of free-jet formation and hydrodynamic description (see for example [20, 21]), we note that the range in $n_0 d_*$ where

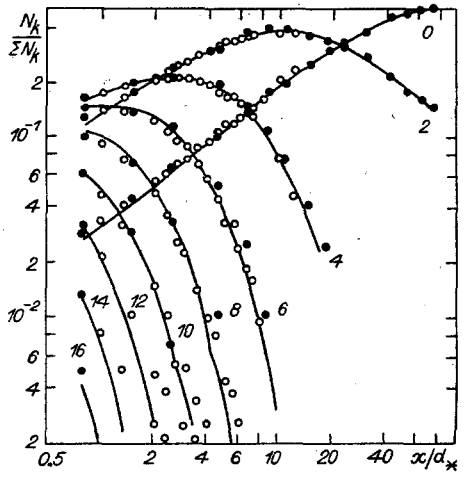

Fig. 4

$I^R_{k'}/I^R_1$ and therefore N_x^X will not vary is the one where that assumption applies. This is confirmed by comparing the isentropic calculations on the N_k^X for a pure nitrogen jet [20] with measurements on N_k^X by Raman scattering [16] for $n_0 d_* = 3.3 \cdot 10^{18}$ cm^{-2}, $T_0 = 290$ K; under those conditions, one expects [20] the equilibrium distribution shown in Fig. 4, which shows also the N_k^X calculated from the 1NS spectra (recorded under the same conditions) with electron-beam diagnosis for the $P^{BX}_{k'k}$. The good agreement confirms that isentropic calculations [18, 20] can be used to determine the equilibrium N_k^X.

3. The $I_{k'}^R$ in the 0–0 band of the 1NS can be measured for known N_k^X for N_2 in the ground state and used with (1.1) and (1.2) to derive the $P^{BX}_{k'k}(E)$, which belongs to the class of ill-posed inverse treatments, which causes difficulties [22]. One cannot determine the $P^{BX}_{k'k}$ matrix from rotational-spectrum measurements alone because the number of unknown elements in $P^{BX}_{k'k}$ is greater than the number of measured $I_{k'}$, and one needs a fairly large set of spectra recorded under independent conditions differing considerably in the equilibrium N_k^X, i.e., it is necessary to make measurements at different gas temperatures.

As the dimensions of the $P^{BX}_{k'k}$ matrix increase, there are tightening specifications for the accuracy in measuring the $I^R_{k'}$, and for correctness in specifying the initial N^X_k distribution. Handling the ill-posed problem can be simplified considerably if there is additional a priori information on the transition probabilities, e.g., the dependence of $P^{BX}_{k'k}$ on k' and k. An effective theoretical method for such transitions excited by fast electrons is provided by the adiabatic approximation [10-12], where the $^1\Sigma$—$^1\Sigma$ transitions have probabilities $P^{BX}_{k'k}$ related by

$$P^{BX}_{k'k}(E) = (2k'+1)\sum_{l=|k'-k|}^{k'+k} P_{l0}(E)\begin{pmatrix} k' & k & l \\ 0 & 0 & 0 \end{pmatrix}^2, \tag{3.1}$$

where $P_{\ell 0}(E)$ is a vector specifying the probabilities of transitions from the zero rotational level in the initial state to rotational level ℓ in the excited state, $\begin{pmatrix} \gamma_1 & \gamma_2 & \gamma_3 \\ m_1 & m_2 & m_3 \end{pmatrix}$ being the Wigner symbol [23]. The expression for the 3_j symbols for $m_1 = m_2 = m_3 = 0$ is [24]

$$\begin{pmatrix} \gamma_1 & \gamma_2 & \gamma_3 \\ 0 & 0 & 0 \end{pmatrix}^2 = \frac{(\gamma_1+\gamma_2-\gamma_3)!\,(\gamma_1-\gamma_2+\gamma_3)!\,(-\gamma_1+\gamma_2+\gamma_3)!}{(\gamma_1+\gamma_2+\gamma_3+1)!} \times \left[\frac{p!}{(p-\gamma_1)!\,(p-\gamma_2)!\,(p-\gamma_3)!}\right]^2, \quad 2p = \gamma_1+\gamma_2+\gamma_3. \tag{3.2}$$

We examined the $^1\Sigma$—$^2\Sigma$, transition, i.e., the excited state was a doublet, but as the splitting of it is very small, the unresolved excited state can be treated as the $^1\Sigma$ state. Then one can use (3.1) for the $P^{BX}_{k'k}$ on the basis that nitrogen molecules in even and odd rotational levels represent different and independent modifications. The $P_{\ell 0}$ for ortho and para nitrogen may in general be different, and denoted by $P^{(+)}_{l0}$ and $P^{(-)}_{l0}$ correspondingly. Also, the only possible transitions are those in which the rotational-state parities change, i.e., k' + k is odd. As the 3_j symbols differ from zero only for even values of k' + k + ℓ, it follows immediately that ℓ in (3.1) can take only odd values.

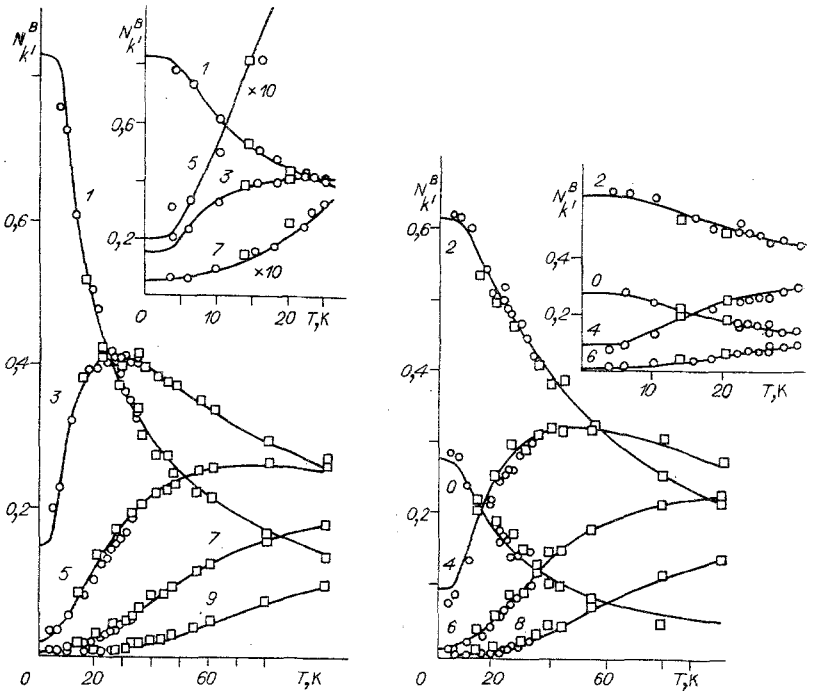

Fig. 5

The $P^{BX}_{k'k}$ matrix is thus expressed via a unique vector $P^{(+)}_{l0}$ for the nitrogen molecules in the even rotational levels k and the vector $P^{(-)}_{l0}$ for the odd levels.

The 3_j symbol normalization condition $\sum_{k'=|k-l|}^{k+l}(2k'+1)\begin{pmatrix} k' & k & l \\ 0 & 0 & 0 \end{pmatrix}^2 = 1$ automatically implies the normalization condition for the $P^{BX}_{k'k}$, if the $P^{(\pm)}_{l0}$: are normalized:

$$\sum_{k'} P^{BX}_{k'k} = \sum_{l} P^{(\pm)}_{l0} \sum_{k'=|k-l|}^{k+l} (2k'+1)\begin{pmatrix} k' & k & l \\ 0 & 0 & 0 \end{pmatrix}^2 = \sum_{l} P^{(\pm)}_{l0} = 1$$

(l takes odd values (l = 1, 3, 5,...). Only $P^{(+)}_{l0}$ has the meaning of the transition probabilities from the zero rotational level, which follows from (3.1) for k = 0 on the basis that

$$(2k'+1)\begin{pmatrix} 0 & k' & l \\ 0 & 0 & 0 \end{pmatrix}^2 = \delta_{k'l}, \text{ i.e., } P^{BX}_{l0} = P^{(+)}_{l0}.$$

$P^{(-)}_{l0}$ does not have that meaning, but it can be related to the probabilities of the transitions from levels l in the ground state to the zero rotational level in the excited state k' = 0: $P^{BX}_{0l} = P^{(-)}_{l0}\begin{pmatrix} 0 & l & l \\ 0 & 0 & 0 \end{pmatrix}^2 = P^{(-)}_{l0}/(2l+1)$. If we assume that $P^{(\pm)}_{l0} = 1$ and $P^{(\pm)}_{l0} = 0$ for $l > 1$, the probabilities $P_{k'k}$ will be equal to the dipole ones with the selection rules $\Delta k = k' - k = \pm 1$:

$$P^{(1)}_{k'k} = \frac{k+1}{2k+1},\ k' = k+1,\ P^{(1)}_{k'k} = \frac{k}{2k+1},\ k' = k-1. \tag{3.3}$$

Such rotational-transition probabilities arise when one incorporates the dipole interaction in the first Born approximation and in particular they describe the probabilities for allowed optical dipole transitions.

In [1] it was suggested by analogy with optical emission and absorption that the (3.3) dipole selection rules apply also on the excitation of nitrogen from the ground state to the $N_2^+(B^2\Sigma_u^+)$ state by electron impact. The [1] has been extensively used in research on nitrogen flows by electron beam methods. However, when the method has been extended to low temperatures and free nitrogen jets, it has been found [24-26] that the (3.3) dipole selection rules do not apply for this process.

TABLE 1

k'	P_{l0}					$\sum_{l=1}^{9} P_{l0}$
	l					
	1	3	5	7	9	
1	0,8251	0,1495	0,01825	0,00192	—0,00015	0,9946
3	0.8259	0,1494	0,01778	0,00180	—0,00003	0,9949
5	0,8278	0,1516	0,01959	0,00217	0,00004	1,0012
7	0,8276	0,1512	0,01876	0,00453	0,00016	1,0023
9	0,8278	0,1516	0,01972	0,00433	0,0013	1,0048
11	0,8279	0,1521	0,02193	0,01229	0,00175	1,0160
$\widehat{P}_{l0}$	0,8277	0,1514	0,01865	0,00199	0,00020	0,9999
σ_l	0,0045	0,0024	0,00093	0,00053	0,00032	—

We used the (3.1) adiabatic approximation to specify the multiquantum rotational-transition probabilities. The input data for $P_{l0}^{(\pm)}$ for the ortho and para forms were provided by measurements on the $I_{k'}^{R}(T_i)$ for the R branch of the 0–0 band with equilibrium distributions. We used 25 spectrograms recorded at isentropic temperatures from 3.9 to 45 K; the $P_{l0}^{(\pm)}$ were determined in two ways, in the first of which we used a set of R-branch intensities $I_{k'}^{R}(T_i)$ for each spectrogram with a fixed T_i separately for even and odd k'.

To solve (1.1) and (1.2) for $P_{\ell 0}$, we used regularization [22], and to improve the accuracy, we used a form where the trial solution was used as the initial approximation, with that solution for $P_{l0}^{(\pm)}$ taken as the one-parameter solution $\widehat{P}_{l0}$, obtained in [25]: $\widehat{P}_{10} = 0.8277$, $\widehat{P}_{30} = 0.1514$, $\widehat{P}_{50} = 0.0187$, $\widehat{P}_{70} = 0.0020$. For each T_i we derived the $P_{l0}^{(\pm)}$ separately for the even and odd rotational levels, and subsequent averaging gave the mean values for $P_{l0}^{(+)}$ and $P_{l0}^{(-)}$: $P_{10}^{(+)} = 0.824 \pm 0.015$, $P_{10}^{(-)} = 0.819 \pm 0.025$, $P_{30}^{(+)} = 0.147 + 0.009$, $P_{30}^{(-)} = 0.150 \pm 0.025$, $P_{50}^{(+)} = 0.019 \pm 0.009$, $P_{50}^{(-)} = 0.022 \pm 0.010$. It is clear that the $P_{10}^{(\pm)}$, $P_{30}^{(\pm)}$ and $P_{50}^{(\pm)}$ for the even and odd levels coincide closely, so we assume below that $P_{l0}^{(+)} = P_{l0}^{(-)} = P_{l0}$. A deficiency in this method of determining the $P_{\ell 0}$ from a particular spectrogram at a given temperature is that the number of input data is relatively small, and therefore there is a stringent requirement for accurate $I_{k'}$ measurement.

In the second method, all the measured intensities were represented as $N_{k'}^{B}(T_i)$ for each k'. The resulting populations $N_{k'}^{B}$ are shown in Figs. 5 and 6 for odd and even k' correspondingly ($\sum_k N_{k'}^{B} = 1$ for even and odd k).

Equation (1.2) has been solved by regularization [22] for each odd k' and the entire T_i set to give $P_{\ell 0}$ by the use of the trial solution from [25], as in the first method. The regularization parameter was derived by maximum likelihood [22]. The spread in the input $N_{k'}^{B}$ for each k' was determined directly from Fig. 5. The $P_{\ell 0}$ calculated for k' = 1, ..., 11 are given in Table 1 together with the trial solutions $\widehat{P}_{l0}$ used and the sums $\sum_l P_{l0}$ for each $P_{\ell 0}$ set. Any difference between such a sum and one is indicative of the accuracy in calculating $P_{\ell 0}$. The trial solutions for ℓ = 1, 3, and 5 are close to those derived by regularization. Also, (1.1) and (1.2) show that the term having ℓ = k' in (1.2) is the dominant one for odd k' for sufficiently low T_i. This is particularly well seen for $T_i \to 0$, where only one level having k = 0 is populated in the ground state and $N_{k=0}^{X} \to 1$. Then the excited-state populations tend to their limiting values:

$$N_{k'}^{B}(T_i) \to \sum P_{l0}(2k'+1)\begin{pmatrix} k' & 0 & l \\ 0 & 0 & 0 \end{pmatrix}^2 = P_{k'0}.$$

The $P_{\ell 0}$ for a given ℓ are best determined by measuring the line intensities for k' = ℓ. These are on the diagonal in Table 1, and the standard deviations σ_ℓ in determining them are shown as a separate line. The sum of the diagonal $P_{\ell 0}$ is 0.99992, which is additional evidence for taking them in calculating the entire $P_{k'k}$ matrix.

The lines in Figs. 5 and 6 give the calculated $N_{k'}^{B}(T_i)$ for odd and even k' based on the selected $P_{\ell 0}$ with (1.2) and (3.1). There is very good agreement with experiment throughout the temperature range, which on the one hand indicates that (3.1) is applicable and on the other confirms that isentropic equilibrium conditions apply in these nitrogen and argon–nitrogen jets for our conditions (for N_2, the isentropic calculation corresponds to the flow in a diatomic gas, while for N_2–Ar, to a monatomic one). The $P_{k'k}$ for even k' (odd k) can be

TABLE 2

k'	$P_{k'k}$					
	k					
	0	2	4	6	8	10
1	0,82506 0,8346 0,8277 1	0,36844 0,3706 0,3700 0,4000	0,03143 0,0310 0,0317 0	0,00295 0,0037 0,0027 0	0,00055 0,0006 — 0	0,00011 0,0001 — 0
3	0,14940 0,1350 0,1514 0	0,54081 0,5384 0,5427 0,6000	0,39746 0,3975 0,3984 0,4444	0,03770 0,0365 0,0377 0	0,00365 0,0045 — 0	0,00066 0,0008 — 0
5	0,01959 0,0233 0,0187 0	0,07763 0,0747 0,0775 0	0,49516 0,4948 0,4963 0,5555	0,41058 0,4105 0,4117 0,4615	0,04064 0,0494 — 0	0,00402 0,0050 — 0
7	0,00453 0,0051 0,0020 0	0,01025 0,0124 0,0088 0	0,06558 0,0635 0,0657 0	0,47855 0,4783 0,4799 0,5385	0,41798 0,4179 — 0,4706	0,04247 0,0412 — 0
9	0,00142 0,0012 — 0	0,00228 0,0026 — 0	0,00813 0,0101 — 0	0,06088 0,0590 — 0	0,47005 0,4698 — 0,5294	0,42268 0,4225 — 0,4783

derived from $(2k+1)P_{k'k} = (2k'+1)P_{kk'}$, which follows from (3.1) and the symmetry conditions for the 3_j symbols.

4. Table 2 compares our $P_{k'k}$, (line 1) with the [26] results, with the one-parameter model [25], and the dipole model [1] (lines 2-4). Multiquantum transitions having $|\Delta k| = |k' - k| > 1$ constitute from 10 to 18% for the various k. This may appear to be a minor difference from the dipole model, but the multiquantum transitions play a considerable part as Fig. 2 shows, if one considers the low gas temperatures. Also, the $P_{k'k}$ for the multiquantum models are similar for $\Delta k = \pm 1, \pm 3$ and appreciable differences set in only for $|\Delta k| \geqslant 5$.

The [25] model resembles ours in being based on (3.1), and in it, it has been assumed for simplicity that the $P_{\ell 0}$ have a one-parameter relationship:

$$P_{l0} = \frac{(2l+1)\alpha^l}{\sum_l (2l+1)\alpha^l} = (2l+1)\alpha^{l-1}\frac{(1-\alpha^2)^2}{(3+\alpha^2)}, \quad l = 1,3,5,\ldots \tag{4.1}$$

Parameter α has been chosen to give the best agreement between the calculations and measurements at the axis on the 1NS rotational line intensities; $\alpha = 0.28 \pm 0.01$, which describes the spectra well. The main disadvantage of this model is that there is no particular basis for (4.1), which is eliminated in our study by the direct calculation of the $P_{\ell 0}$.

The $\ln [P_{l0}/(2l+1)]$ as functions of ℓ can be compared for the $P_{\ell 0}$ corresponding to the diagonal values in Table 1; this shows that the probabilities are closely described by (4.1) for $\ell = 1$, 3, and 5. The slope of the straight line gives $\alpha = 0.278$. This line also passes closely through the origin, i.e., the normalization factor in (4.1) is one:

$$\sum_l (2l+1)\alpha^l = \alpha(3+\alpha^2)/(1-\alpha^2)^2 = 1. \tag{4.2}$$

This also enables one to determine α: $\alpha_0 = 0.27704127$, so from (4.2) the probabilities are $P_{\ell 0} \simeq (2\ell+1)\exp(-\delta\ell)$ ($\delta = -\ln \alpha_0 = 1.283588$).

Most of the measurements used here were made on exciting the nitrogen with electrons at 10-20 keV; the measured relative distributions were independent of the electron energy under unaltered conditions, but measurements at the edge of the electron beam [6], where the N_2 is excited mainly by secondary electrons whose energy is close to the threshold for exciting the $N_2^+(B^2\Sigma_u^+)$ state (E ≈ 18.7 eV), showed that the rotational transition probabilities $\langle P_{k'k}^{BX} \rangle$

for such electrons differ substantially from the $P^{BX}_{k'k}$ for fast primary ones. For example, the $P_{\ell 0}$ for 10-20 keV electrons defined $\alpha = 0.28$, whereas $\alpha = 0.56$ for the secondary electrons [6]; so the slow electrons transfer much more momentum.

The energy dependence in $P^{BX}_{k'k}(E)$ can be derived from measurements on the rotational energies of the $N_2^+(B^2\Sigma_u^+)$ ions for fixed rotational energy in the $N_2(X^1\Sigma_u^+)$ molecules. The rotational energy of a molecule in the ground state in degrees is $E_R^X = \Theta^X \sum_k N_k^X k(k+1)$ while in the state excited by electron impact, that energy E_R^B can be represented by means of the $P_{k'k}$ as $E_R^B = \Theta^B \sum_{k'} N_{k'}^B k'(k'+1) = \Theta^B \sum_{k'} k'(k'+1) \sum_k P_{k'k} N_k^X =$

$$= \Theta^B \sum_{k'} k'(k'+1)(2k'+1) \sum_k N_k^X \sum_l P_{l0} \begin{pmatrix} k & k' & l \\ 0 & 0 & 0 \end{pmatrix}^2. \quad (4.3)$$

The relation $\sum_{k'} k'(k'+1)(2k'+1) \begin{pmatrix} k & k' & l \\ 0 & 0 & 0 \end{pmatrix}^2 = k(k+1) + l(l+1)$ for the 3_j symbols [24] can be used with (4.3) to derive $E_R^B = \Theta^B \sum_k N_k^X \sum_l P_{l0}[k(k+1) + l(l+1)]$, so the normalization of N_k^X and $P_{\ell 0}$ gives

$$E_R^B = \frac{\Theta^B}{\Theta^X} E_R^X + \Theta^B \sum_l P_{l0} l(l+1). \quad (4.4)$$

Here

$$\Delta\varepsilon^{XB} = \Theta^B \sum_l P_{l0}(E)\, l(l+1)$$

defines the additional rotational-energy transfer through the molecule on electron impact. In the adiabatic approximation, $\Delta\varepsilon^{XB}$ is independent of the rotational distribution in the initial state but may be dependent on the electron energy.

At high temperatures and close to equilibrium, $E_R^X \approx T_R^X$, $E_R^B \approx T_R^B$, and if $T_R^X \gg \Delta\varepsilon^{XB}$, then (4.4) becomes $T_R^B \approx (\Theta^B/\Theta^X) T_R^X$, which is used widely for low-temperature plasmas to derive the gas temperature from measurements on excited-molecule temperatures [9, 27, 28].

Molecular nitrogen excited by 10-20 keV electrons has heating $\Delta\varepsilon^{XB} = (4.4 \pm 0.8)\Theta^X = (12.7 \pm 0.9)$K as calculated from the $P_{\ell 0}$ in Table 2, while for the dipole model ($P_{\ell 0} = 1$), no matter what the electron energy, $\Delta\varepsilon^{XB} = 2\Theta^X \approx 5.8$ K, which is a result obtained in [6, 29].

As $\Delta\varepsilon^{XB}$ is independent of the population distribution, one can calculate the rotational energy in the $N_2(X^1\Sigma_g^+)$ state without extracting the level populations for that state from spectrograms.

In [7], the rotational temperature was derived for $N_2^+(B^2\Sigma_u^+)$ in a jet of nitrogen or argon containing a little N_2 on excitation by electrons with energies from 20 to 600 eV. The system [7] in general was the same as ours. The measurements showed that T_R^B was independent of electron energy above 100-150 eV, while below 150 eV down to close to the threshold, T_R^B and E_R^B increased by about 10 K, so $\Delta\varepsilon^{XB}$ near the threshold for excitation of the $N_2^+(B^2\Sigma_u^+)$ state is about $(8 \pm 1)\Theta^X$, i.e., about 20-25 K.

This approach to electron-impact excitation for nitrogen can be applied to other substances, as the main advantage is that a free jet is used as a low-temperature gas target having a known rotational-level population distribution.

We are indebted to N. V. Karelov for participating in the early experiments.

LITERATURE CITED

1. E. P. Muntz, "Static temperature measurements in a flowing gas," Phys. Fluids, 5, No. 1 (1962).
2. G. Herzberg, Molecular Spectra and Molecular Structure. 1. Spectra of Diatomic Molecules, Van Nostrand, New York (1950).
3. A. D. Sakharov, "Excitation temperatures in gas-discharge plasmas", Izv. AN SSSR, Ser. Fiz., 12, No. 4 (1948).
4. D. K. Otorbaev, V. N. Ochkin, et al., "Large momentum transfer in electron excitation of molecules", Pis'ma Zh. Éksp. Teor. Fiz., 28, No. 6, (1978).
5. A. E. Belikov, N. V. Karelov, A. K. Rebrov, and R. G. Sharafutdinov, "Electron-beam measurements: secondary processes in $B^2\Sigma_u^+$ excitation for nitrogen ions", Low-Density Gas Flow Diagnosis [in Russian], Novosibirsk (1979).

6. G. I. Sukhinin and R. G. Sharafutdinov, "Determining effective rotational-transition probabilities in electron-impact excitation of the $N_2^+ B^2\Sigma_u^+ v', k'$ state from the nitrogen $N_2 X^1\Sigma_g^+, v = 0, k$ ground state," Zh. Tekhn. Fiz., 53, No. 2 (1982).
7. B. M. De Koven, H. H. Harris, et al., "Rotational excitation in the electron impact ionization of supercooled N_2", J. Chem. Phys., 74, No. 10 (1981).
8. S. P. Hernandes, P. J. Dagdigian, and J. P. Doering, "Experimental verification of the breakdown of the electric dipole rotational selection rule in electron impact ionization-excitation of N_2", J. Chem. Phys., 77, No. 12 (1982).
9. B. P. Lavrov, "Electronic-rotational diatomic-molecule spectra and nonequilibrium-plasma diagnosis", Plasma Chemistry [in Russian], Atomenergoizdat, Moscow (1984), No. 11.
10. S. J. Chu and A. Dalgarno, "The rotational excitation of carbon monoxide by hydrogen atom impact", Proc. Royal Society, A342, No. 1629 (1975).
11. R. Goldflam, S. Green, and D. J. Kouri, "Infinite order sudden approximation for rotational energy transfer in gaseous mixtures", J. Chem. Phys., 67, No. 9 (1977).
12. P. L. Rubin, "Rotational-level population probabilities in the electron excitation of diatomic molecules", Zh. Éksp. Teor. Fiz., 65 (1973).
13. B. N. Borzenko, N. V. Karelov, et al., "Measurements on rotational-level populations for a free nitrogen jet", Zh. Prikl. Mat. Tekhn. Fiz., No. 5 (1976).
14. A. K. Rebrov, G. I. Sukhinin, et al., "Electron-beam diagnosis for nitrogen: secondary processes", Zh. Tekhn. Fiz., 51, No. 9 (1981).
15. H. Helvajian, B. M. De Koven, and A. P. Baronavski, "Laser-induced fluorescence of $N_2(X^1\Sigma_g^+)$ and electron-impact excited $N_2^+(X^2\Sigma_g^+)$ in a pulsed supersonic beam: rotational distributions", Chem. Phys., 90, No. 1 (1984).
16. G. Luijks, S. Stolte, and J. Reuss, "Molecular beam diagnostics by Raman scattering", Chem. Phys., 62, No. 2 (1981).
17. P. Huber-Wächli, P. M. Cuthals, and J. W. Nibler, "CARS spectra of supersonic molecular beams", Chem. Phys. Lett., 67, No. 2, 3 (1979).
18. P. A. Skovorodko, "Rotational relaxation in expansion into vacuum", Low-Density Gas Dynamics [in Russian], Novosibirsk (1976).
19. N. V. Karelov, A. K. Rebrov, and R. G. Sharafutdinov, "Rotational-level populations in nonequilibrium condensation in a freely expanding gas", Zh. Prikl. Mat. Tekhn. Fiz., No. 3 (1978).
20. P. A. Skovorodko and R. G. Sharafutdinov, "Rotational-level population kinetics in a free nitrogen jet", Zh. Prikl. Mat. Tekhn. Fiz., No. 5 (1981).
21. H. R. Murphy and D. R. Miller, "Effects of nozzle geometry on kinetics in free-jet expansion", J. Chem. Phys., 88, No. 20 (1984).
22. Yu. E. Voskoboinikov, N. G. Preobrazhenskii, and A. I. Sedel'nikov, Mathematical Measurement Processing in Molecular Gas Dynamics [in Russian], Nauka, Novosibirsk (1984).
23. L. D. Landau and E. M. Lifshits, Quantum Mechanics: Nonrelativistic Theory [in Russian], Fizmatgiz, Moscow (1963).
24. N. Smith and D. E. Pritchard, "Simple analytical approximations based on the energy corrected sudden scaling laws", J. Chem. Phys., 74, No. 7 (1981).
25. A. E. Belikov, A. E. Zarvin, et al., "Electron-beam nitrogen diagnosis: multiquantum rotational transitions on excitation", Zh. Prikl. Mat. Tekhn. Fiz., No. 3 (1984).
26. D. Coe, F. Robben, et al., "Rotational temperatures in nonequilibrium free jet expansion of nitrogen", Phys. Fluids, 23, No. 4 (1980).
27. A. P. Bryukhovetskii, E. N. Kotlikov, et al., "Vibronic-level excitation in hydrogen by electron impact in a nonequilibrium arc-discharge plasma", Zh. Éksp. Teor. Fiz., 79, No. 5 (1980).
28. V. P. Lavrov, V. N. Ostrovskii, and V. I. Ustimov, "The mechanism producing nonequilibrium rotational-level populations in a plasma", Zh. Tekhn. Fiz., 50, No. 10 (1980).
29. P. Schelby and R. A. Hill, "Noniterative method for computing rotational temperatures from electron beam excited nitrogen fluorescence", J. Phys. Fluids, 14, No. 11 (1971).